Supplementary Information

A leap in quantum efficiency through light harvesting in photoreceptor UVR8

Li et al.

Supplementary Methods

Model simulation of picosecond resolved TCSPC transients

1. Simulation of Excited State Population Evolution of Three W Groups

The time evolution of excited state populations of UVR8 tryptophan residues were numerically simulated (from 0 to 30 ns, 4 ps interval) based on kinetic models. Parameters are shown in Supplementary Tables 2, 15 and 16. The RET time constants from QM/MM calculations in Supplementary Table 3 and Fig. 3d were also needed.

Since W_d has two lifetimes, for each W_d, the excited state population was treated as the sum of two subpopulations with the same energy-transfer rate but with distinct lifetimes (Supplementary equation 1), 0.5 ns for W_d1 and 2.7 ns for W_d2. Knowing all lifetimes, excitation energy-transfer total rates (see equation 17) and absorbance values (Fig. 1e and Supplementary Table 5), the differential equations and corresponding boundary conditions describing the population evolution of a distal tryptophan Wm (m=39, 92, 144, 196, 300 or 352) are shown as below:

$$[Wm]_t = [Wm_1]_t + [Wm_2]_t \tag{1}$$

$$\frac{d[Wm_1]_t}{dt} = -(\tau_{total,Wm}{}^{-1} + \tau_1{}^{-1})[Wm_1]_t \qquad [Wm_1]_{t=0} = A_d(\lambda)(1-R_{D2}) \tag{2}$$

$$\frac{d[Wm_2]_t}{dt} = -(\tau_{total,Wm}{}^{-1} + \tau_2{}^{-1})[Wm_2]_t \qquad [Wm_2]_{t=0} = A_d(\lambda)R_{D2} \tag{3}$$

Supplementary equations 2 and 3 define the decay dynamics of the 0.5 ns and 2.7 ns components, respectively, and they are single exponential decays. In the equations, $\tau_{total,Wm}$ is the theoretical total RET time constant (Fig. 2k) calculated using equation 17 for Wm (m=39, 92, 144, 196, 300 or 352). τ_1 and τ_2 are the two lifetimes of W_d, which are 0.5 ns and 2.7 ns, respectively. R_{D2} is the fraction of amplitude for the 2.7 ns lifetime, which is 0.71 as determined by femtosecond fluorescence up-conversion (Fig. 2a). The initial populations are based on normalized W_d absorption spectrum ($A_d(\lambda)$ values, Supplementary Table 5, Fig. 1e) at the excitation wavelength λ (λ=290 nm or 310 nm). The decay curves of all W_d were then added together to obtain the total dynamics of distal tryptophan group:

$$[W_d]_t = [W39]_t + [W92]_t + [W144]_t + [W196]_t + [W300]_t + [W352]_t \tag{4}$$

For each peripheral tryptophan residues Wi (i=198, 250 or 302), depending on the lifetime and energy transfer rates, the total excited population was divided into 4 subpopulations: (1) short lifetime (1-2 ns) and fast energy transfer to $4W_c$, (2) long lifetime (6-8 ns) and fast energy transfer to $4W_c$, (3) short lifetime and slow energy transfer to $4W_c$, (4) long lifetime and slow energy transfer to $4W_c$.

$$[Wi]_t = [Wi_1]_t + [Wi_2]_t + [Wi_3]_t + [Wi_4]_t \tag{5}$$

Each subpopulation has a distinct differential equation and boundary conditions for numerical simulation:

$$\frac{d[Wi_1]_t}{dt} = -(\tau_{total1,Wi}{}^{-1} + \tau_{1,Wi}{}^{-1})[Wi_1]_t + (1-R_{slow,Wi})(1-R_{2,Wi})\sum_{m}^{W_d}(\tau_{RET,WmWi}{}^{-1} + \tau_{RET,WmWi(b)}{}^{-1})[Wm]_t$$

$$[Wi_1]_{t=0} = A_p(\lambda)(1-R_{slow,Wi})(1-R_{2,Wi}) \tag{6}$$

$$\frac{d[Wi_2]_t}{dt} = -(\tau_{total1,Wi}^{-1} + \tau_{2,Wi}^{-1})[Wi_2]_t + (1-R_{slow,Wi})R_{2,Wi}\sum_m^{W_d}(\tau_{RET,WmWi}^{-1} + \tau_{RET,WmWi(b)}^{-1})[Wm]_t$$

$$[Wi_2]_{t=0} = A_p(\lambda)(1-R_{slow,Wi})R_{2,Wi} \quad (7)$$

$$\frac{d[Wi_3]_t}{dt} = -(\tau_{total2,Wi}^{-1} + \tau_{1,Wi}^{-1})[Wi_3]_t + R_{slow,Wi}(1-R_{2,Wi})\sum_m^{W_d}(\tau_{RET,WmWi}^{-1} + \tau_{RET,WmWi(b)}^{-1})[Wm]_t$$

$$[Wi_3]_{t=0} = A_p(\lambda)R_{slow,Wi}(1-R_{2,Wi}) \quad (8)$$

$$\frac{d[Wi_4]_t}{dt} = -(\tau_{total2,Wi}^{-1} + \tau_{2,Wi}^{-1})[Wi_4]_t + R_{slow,Wi}R_{2,Wi}\sum_m^{W_d}(\tau_{RET,WmWi}^{-1} + \tau_{RET,WmWi(b)}^{-1})[Wm]_t$$

$$[Wi_4]_{t=0} = A_p(\lambda)R_{slow,Wi}R_{2,Wi} \quad (9)$$

Supplementary equations 6, 7, 8 and 9 describe the temporal evolution of the 4 excited state subpopulations, respectively. On the right side of each equation, the first term gives the decay due to lifetime decay and energy transfer to W_c; the second term defines the population increase kinetics due to energy transfer from W_d. In the above equations, $\tau_{total1,Wi}$ and $\tau_{total2,Wi}$ are the fast and slow QM/MM total RET time constant from peripheral tryptophan Wi (i=198, 250 or 302) to the 4 pyramid center tryptophan residues (shown in Fig. 3d). $\tau_{1,Wi}$ and $\tau_{2,Wi}$ are the two lifetimes of Wi. $\tau_{RET,WmWi}$ is the RET time constant from one distal tryptophan Wm to the peripheral tryptophan Wi and $\tau_{RET,WmWi(b)}$ is the RET time constant from the same W_d to the W_p on the other subunit (Supplementary Table 3). $[Wm]_t$ is the population evolution of excited distal tryptophan m (m=39, 92, 144, 196, 300 or 352) simulated as above mentioned. $R_{2,Wi}$ is the fraction of amplitude for the longer lifetime (6-8 ns) and $R_{slow,Wi}$ stands for the population ratio of W_p with slow transfer energy to W_c (shown in Fig. 3d). $A_p(\lambda)$ is the value of the normalized W_p absorption spectrum (shown in Fig. 1e and Supplementary Table 5) at the excitation wavelength λ (λ=290 nm or 310 nm), which determines initial population of W_p. For W_p that were knocked out in the mutant, the $A_p(\lambda)$ value was set to 0. For each mutant, the simulated transients for peripheral tryptophan residues present in the mutant were added together to give the total dynamics of peripheral tryptophan group:

$$[W_p]_t = \sum_i [Wi]_t \quad (10)$$

Our model treated the 4 pyramid center tryptophan residues ($4W_c$) as a whole. Since 2 decay time constants were observed (0.08 ns and 1.4 ns) for the pyramid center, we divide W_c into two subpopulations:

$$[W_c]_t = [W_{c1}]_t + [W_{c2}]_t \quad (11)$$

$$\frac{d[W_{c1}]_t}{dt} = -\tau_{c1}^{-1}[W_{c1}]_t + R_{c1}\sum_m^{W_d}\sum_n^{W_c}(\tau_{RET,WmWn}^{-1} + \tau_{RET,WmWn(b)}^{-1})[Wm]_t + R_{c1}\sum_i^{W_p}\tau_{total1,Wi}^{-1}([Wi_1]_t + [Wi_2]_t)$$

$$+R_{c1}\sum_i^{W_p}\tau_{total2,Wi}^{-1}([Wi_3]_t + [Wi_4]_t)$$

$$[W_{c1}]_{t=0} = 4A_c(\lambda)R_{c1} \quad (12)$$

$$\frac{d[W_{c2}]_t}{dt} = -{\tau_{c2}}^{-1}[W_{c2}]_t + (1-R_{c1})\sum_m^{W_d}\sum_n^{W_c}({\tau_{RET,WmWn}}^{-1} + {\tau_{RET,WmWn(b)}}^{-1})[Wm]_t$$

$$+(1-R_{c1})\sum_i^{W_p}{\tau_{total1,Wi}}^{-1}([Wi_1]_t + [Wi_2]_t) + (1-R_{c1})\sum_i^{W_p}{\tau_{total2,Wi}}^{-1}([Wi_3]_t + [Wi_4]_t)$$

$$[W_{c2}]_{t=0} = 4A_c(\lambda)(1-R_{c1}) \tag{13}$$

In Supplementary equations 12 and 13, τ_{c1} and τ_{c2} are the two fluorescence decay times of the pyramid center, which are 0.08 ns and 1.4 ns, respectively. $\tau_{RET,WmWn}$ and $\tau_{RET,WmWn(b)}$ are the RET time constants from one distal tryptophan Wm (m=39, 92, 144, 196, 300 or 352) to the pyramid center tryptophan Wn on the same and on the other subunit (Supplementary Table 3), respectively. $[Wm]_t$ is the kinetics of excited distal tryptophan m (m=39, 92, 144, 196, 300 or 352) simulated as above mentioned. $\tau_{total1,Wi}$ and $\tau_{total2,Wi}$ are the fast and slow QM/MM total RET time constant from peripheral tryptophan Wi (i=198, 250 or 302) to the 4 pyramid center tryptophan residues (Fig. 3d). $[Wi_1]_t$, $[Wi_2]_t$, $[Wi_3]_t$ and $[Wi_4]_t$ are the temporal evolutions of the four subpopulations (as above mentioned) of peripheral tryptophan Wi. R_{c1} is the amplitude ratio of the 80 ps component, which is 0.75. $A_c(\lambda)$ is the value of the normalized W_c absorption spectrum (Supplementary Table 5, shown in Fig. 1e) at the excitation wavelength λ (λ=290 nm or 310 nm). Simulations were conducted for W198F, W250F and W198/250F at 310-nm excitation; and WT at 310-nm and 290-nm excitation. Simulated tryptophan excited state temporal evaluation of WT (290 nm excitation) is shown in Supplementary Fig. 16 as an example.

2. Simulation of Fluorescence Transients and Contributions from Three Tryptophan Groups

The total simulated signal (Simul.) was given by the sum of contributions from W_d, W_p and W_c:

$$Simul.(t) = S(W_d) + S(W_p) + S(W_c) \tag{14}$$

Three groups have different emission rates and thus have different weights in the total signal. The instrument response of TCSPC also needs to be considered. Therefore, the contributions were calculated using the following equations:

$$S(W_d) = A \bullet FL_d(\lambda)\int_{-\infty}^{+\infty} IRF(\tau)[W_d]_{t-\tau}d\tau \tag{15}$$

$$S(W_p) = A \bullet FL_p(\lambda)\int_{-\infty}^{+\infty} IRF(\tau)[W_p]_{t-\tau}d\tau \tag{16}$$

$$S(W_c) = A \bullet FL_c(\lambda)\int_{-\infty}^{+\infty} IRF(\tau)[W_c]_{t-\tau}d\tau \tag{17}$$

where $[W_d]$, $[W_p]$ and $[W_c]$ are the kinetics of excited distal, peripheral and pyramid center tryptophan chromophores as defined in Supplementary equations 4, 10 and 11, respectively. IRF is the instrument response function as recorded using buffer scattering (Supplementary Fig. 15a). FL_d, FL_p and FL_c are the fluorescence intensity of W_d, W_p and W_c per unit population per unit time, respectively, giving different signal weights to 3 W groups. FL_d, FL_p and FL_c have the same spectra shapes as fluorescence spectra shown in Fig. 1e, but with different absolute intensities

(Supplementary Table 19), which were determined by fluorescence QY and lifetimes of 3 W groups (Supplementary Fig. 15). For comparison with experimental data, a common normalizing factor (A) was applied to Supplementary equations 15, 16 and 17 to give a normalized total simulation curve without affecting the dynamics.

For different mutants, picosecond resolved TCSPC data at multiple fluorescence wavelengths were simulated using our model (Supplementary Figs. 9-13). Given the fact that the steady-state emission is the sum of time integrals of time-resolved fluorescence from 3 W groups (Supplementary equation 18), with the steady-state emission spectra of the mutant and simulation data at various fluorescence wavelengths, the spectra of W_d, W_p and W_c can be determined by decomposing the steady-state emission.

$$I(\lambda) = I_d(\lambda) + I_p(\lambda) + I_c(\lambda) \tag{18}$$

$$I_d(\lambda) = I(\lambda)\frac{\int_0^{+\infty} FL_d(\lambda)[W_d]_t\,dt}{\int_0^{+\infty} FL_d(\lambda)[W_d]_t\,dt + \int_0^{+\infty} FL_p(\lambda)[W_p]_t\,dt + \int_0^{+\infty} FL_c(\lambda)[W_c]_t\,dt} \tag{19}$$

$$I_p(\lambda) = I(\lambda)\frac{\int_0^{+\infty} FL_p(\lambda)[W_p]_t\,dt}{\int_0^{+\infty} FL_d(\lambda)[W_d]_t\,dt + \int_0^{+\infty} FL_p(\lambda)[W_p]_t\,dt + \int_0^{+\infty} FL_c(\lambda)[W_c]_t\,dt} \tag{20}$$

$$I_c(\lambda) = I(\lambda)\frac{\int_0^{+\infty} FL_c(\lambda)[W_c]_t\,dt}{\int_0^{+\infty} FL_d(\lambda)[W_d]_t\,dt + \int_0^{+\infty} FL_p(\lambda)[W_p]_t\,dt + \int_0^{+\infty} FL_c(\lambda)[W_c]_t\,dt} \tag{21}$$

where $I(\lambda)$ is the total steady-state emission spectrum. The shapes of resulted I_d, I_p and I_c (Fig. 3l-o colored symbols) agree well with directly measured emission spectra of W_d, W_p and W_c groups, which further validates our energy transfer model.

Overall RET efficiency of UVR8

Details about FRET efficiency calculations can be found elsewhere[1]. Briefly, RET efficiency (E) can be calculated with donor lifetimes with and without acceptors:

$$E = 1 - \frac{\tau_{DA}}{\tau_D} \tag{22}$$

where τ_{DA} and τ_D are donor fluorescence decay times with and without the acceptors respectively. In our study, τ_D was experimentally measured when the acceptors were removed by site-directed mutagenesis. τ_{DA} was calculated using τ_D and theoretically calculated total RET rates τ_{total} (defined in equation 17):

$$\tau_{DA} = \frac{1}{{\tau_D}^{-1} + {\tau_{total}}^{-1}} \tag{23}$$

Equations 21 and 22 were readily obtained with Supplementary equations 22 and 23.

For WT, the energy transfer efficiency from W_d directly to the pyramid center ($4W_c$) was

calculated for each W_d.

$$E_{direct,Wm4W_c} = E_{Wm}\frac{R_{Wm}}{R_{Wm}+1} \tag{24}$$

E_{Wm} is the RET efficiency for Wm (m=39, 92, 144, 196, 300 or 352) in WT as calculated with equation 20. R_{Wm} is the RET branching ratio of direct transfer for Wm shown in Supplementary Table 3.

The energy transfer efficiency from each W_d to certain W_p was calculated as follows:

$$E_{WmWi} = E_{Wm}\frac{\tau_{RET,WmWi}^{-1} + \tau_{RET,WmWi(b)}^{-1}}{\tau_{total,Wm}^{-1}} \tag{25}$$

$\tau_{total,Wm}$ is the QM/MM total RET time constant defined in equation 14 (shown in Fig. 2k) for Wm (m=39, 92, 144, 196, 300 or 352). $\tau_{RET,WmWi}$ and $\tau_{RET,WmWi(b)}$ are the RET time constants for D-A pairs Wm-Wi and Wm-Wib (i=198, 250 or 302) respectively (data shown in Supplementary Table 3).

The energy transfer efficiency from each W_d to the pyramid center via two-step transfer through W_p was calculated using the following equation:

$$E_{twostep,Wm4W_c} = E_{W198}E_{WmW198} + E_{W250}E_{WmW250} + E_{W302}E_{WmW302} \tag{26}$$

E_{W198}, E_{W250} and E_{W302} are the energy transfer efficiencies to the pyramid center given by equation 24. E_{WmW198}, E_{WmW250} and E_{WmW302} are the energy transfer efficiencies from Wm (m=39, 92, 144, 196, 300 or 352) to W198, W250 and W302 respectively, calculated using Supplementary equation 25.

Total efficiencies for W_d energy transfer to the pyramid center is the sum of efficiencies of the direct and indirect transfer.

$$E_{Wm4W_c} = E_{direct,Wm4W_c} + E_{twostep,Wm4W_c} \tag{27}$$

All results are shown in Supplementary Table 4.

Finally, the fraction of absorbed photons (λ_{ex}=290 nm) that is ultimately utilized to excite the pyramid center in UVR8 WT was given by the following equation:

$$E_{290nm} = \frac{A_d(290nm)\sum_m^{W_d} E_{Wm4W_c} + A_p(290nm)\sum_i^{W_p} E_{Wi} + 4A_c(290nm)}{6A_d(290nm) + 3A_p(290nm) + 4A_c(290nm)} \tag{28}$$

By plugging in the efficiency values in Supplementary Table 4 and absorbance values in Supplementary Table 5, the light harvesting efficiency in UVR8 was calculated as follows:

$$E_{290nm} = \frac{0.668\times(0.34+0.37+0.49+0.35+0.52+0.51)+0.846\times(0.63+0.94+0.96)+4\times0.888}{6\times0.668+3\times0.846+4\times0.888} = 0.73 \tag{29}$$

meaning that for every 100 photons absorbed by UVR8 WT, about 73 of them finally reach the pyramid center. If all energy transfer efficiencies (E) are set to zero, Supplementary equation 28 gives the probability of direct excitation of the pyramid center, which is 0.35, indicating the energy transfer network increases the light perception efficiency from 35% to 73%.

The total efficiency of the 80 ps photoreaction channel (λ_{ex}=290 nm) is:

$$E_Q = R_{c1}E_{290nm} = 0.75\times0.73 = 0.55 \tag{30}$$

With R_{c1}=0.75, E_Q was calculated to be 0.55, suggesting that for every 100 photons absorbed by UVR8 WT, about 55 of them were quenched via the 80 ps channel.

Supplementary Figures

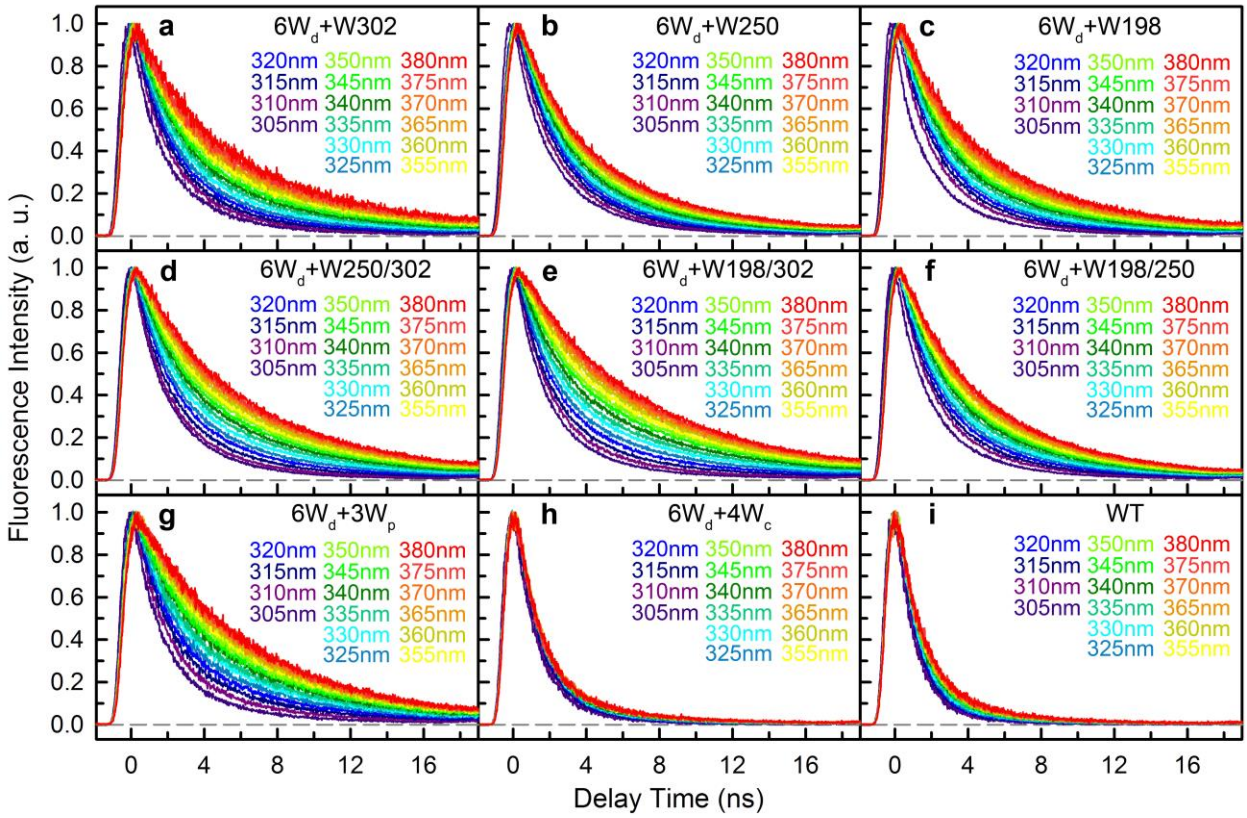

Supplementary Figure 1 | Fluorescence decay transients (λ_{ex}=290 nm) from 305 nm to 380 nm for UVR8 WT and 8 mutants measured with sub-nanosecond-resolved time correlated single photon counting (TCSPC). **a**, 4W$_c$/198/250F (6W$_d$+W302). **b**, 4W$_c$/198/302F (6W$_d$+W250). **c**, 4W$_c$/250/302F (6W$_d$+W198). **d**, 4W$_c$/198F (6W$_d$+W250/302). **e**, 4W$_c$/250F (6W$_d$+W198/302). **f**, 4W$_c$/302F (6W$_d$+W198/250). **g**, 6W$_d$+3W$_p$. **h**, 6W$_d$+4W$_c$. **i**, WT.

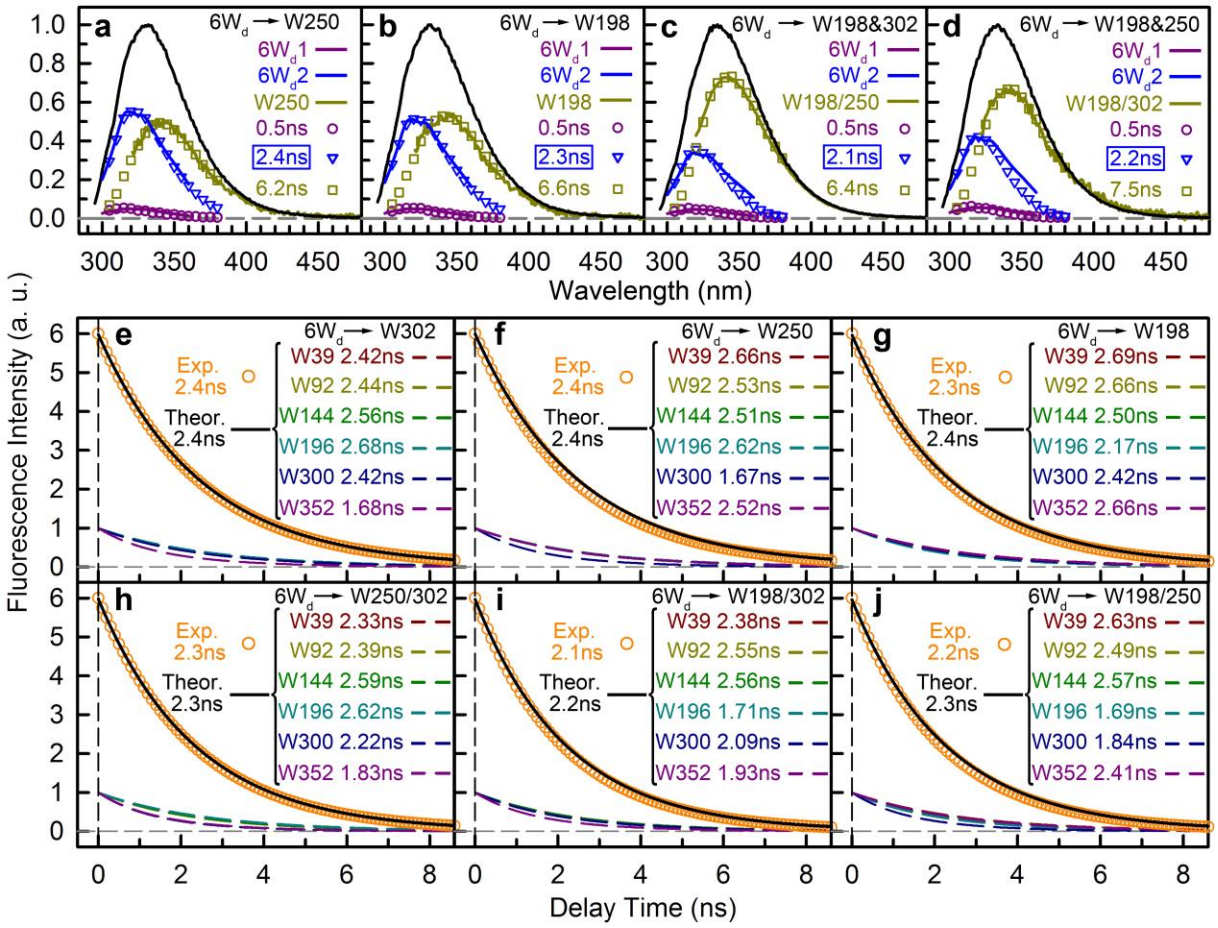

Supplementary Figure 2 | Excitation energy transfer from W_d to W_p and W_c. a-d, Time scales from a global fitting and lifetime-associated spectra of $6W_d$+W250 (**a**), $6W_d$+W198 (**b**), $6W_d$+W198 & W302 (**c**) and $6W_d$+W198 & W250 (**d**). For each panel, the black solid lines are the steady-state emission spectra of the protein samples. The lifetime-associated spectra are shown in various symbols and the directly measured spectra are shown in lines. **e-j**, Model simulations demonstrate that the total fluorescence decay dynamics of the $6W_d$ in UVR8 can be described with single exponential decays in the following UVR8 protein samples: $4W_c$/198/250F (**e**), $4W_c$/198/302F (**f**), $4W_c$/250/302F (**g**), $4W_c$/198F (**h**), $4W_c$/250F (**i**), $4W_c$/302F (**j**). In each panel, the 6 dashed lines correspond to the simulated single exponential decays of the original 2.7-ns component based on experimental τ_2 (2.7 ns) and theoretical total RET times (τ_{total}) for W39 (dark red), W92 (dark yellow), W144 (green), W196 (dark cyan), W300 (dark blue) and W352 (dark purple) respectively. The simulated total decay dynamics of the $6W_d$ (black solid lines, sum of the 6 dashed lines) can be fitted with a single decay time constant (shown in black), which agrees well with experimental dynamics (yellow circles), indicating that FRET theory provides accurate description of the energy transfer processes from W_d in UVR8.

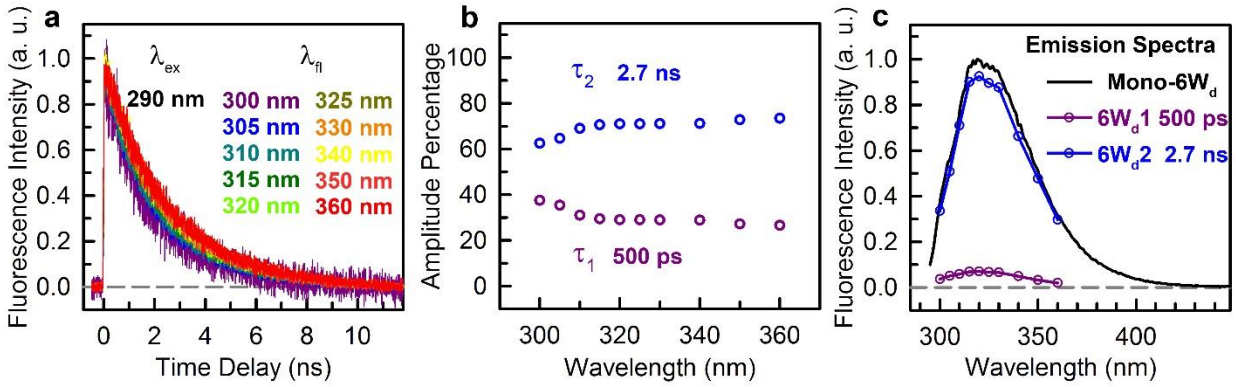

Supplementary Figure 3 | Lifetime-associated spectra of W_d. a, Fluorescence transients (290 nm excitation) of mono-$6W_d$ measured by picosecond-resolved TCSPC. For each plot, the corresponding fluorescence wavelength is labeled with the same color. **b**, Amplitude percentages of 0.5 ns and 2.7 ns lifetimes at different fluorescence wavelengths as determined by biexponential fitting of the fluorescence transients in **a**. **c**, Lifetime-associated spectra of 0.5 ns ($6W_d1$) and 2.7 ns ($6W_d2$) time constants.

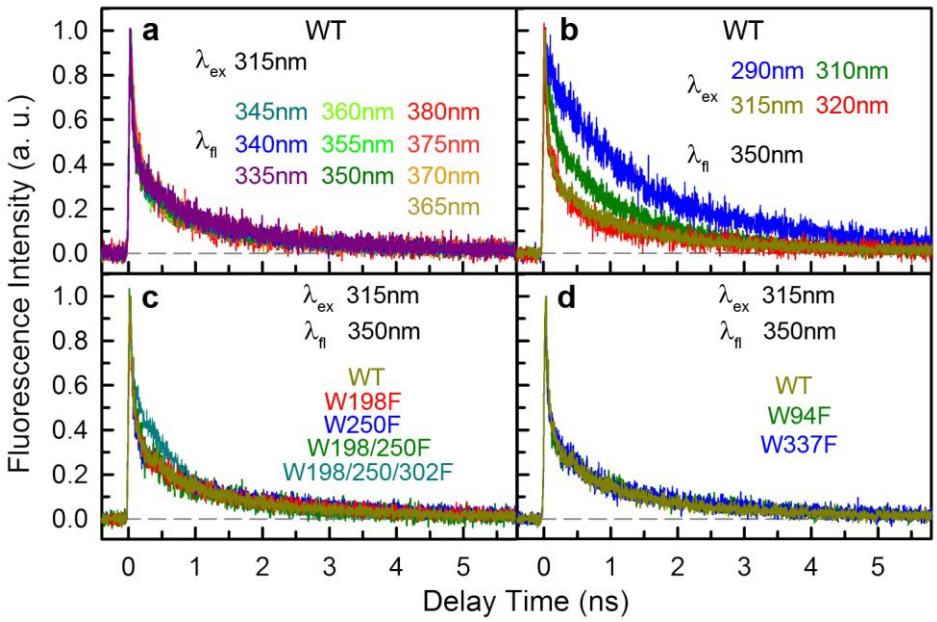

Supplementary Figure 4 | Fluorescence decay transients measured with picosecond resolved TCSPC. a, Decay transients at various fluorescence wavelengths for WT (λ_{ex}=315 nm). All the transients are similar. **b**, Decay transients at 350 nm with various excitation wavelengths (λ_{ex}=290 nm, 310 nm, 315 nm and 320 nm) for WT. Fluorescence decay signals with 315 nm and 320 nm excitation wavelengths gives pure pyramid center ($4W_c$) dynamics. In addition to $4W_c$ dynamics, 310 nm excitation transients also have contributions from $3W_p$; 290 nm excitation transients contain dynamics of all three groups. **c**, Fluorescence dynamics of the pyramid center measured by 315 nm excitation, for WT (dark yellow), W198F (red), W250F (blue), W198/250F (green) and W198/250/302F ($6W_d$+$4W_c$, cyan). All transients are similar except that for W198/250/302F ($6W_d$+$4W_c$), indicating that mutation of W302 affects the pyramid center fluorescence dynamics and gives an extra 5.4-ns slow decay constant. **d**, Fluorescence dynamics of the pyramid center measured by 315 nm excitation for WT, W94F and W337F. All transients are similar.

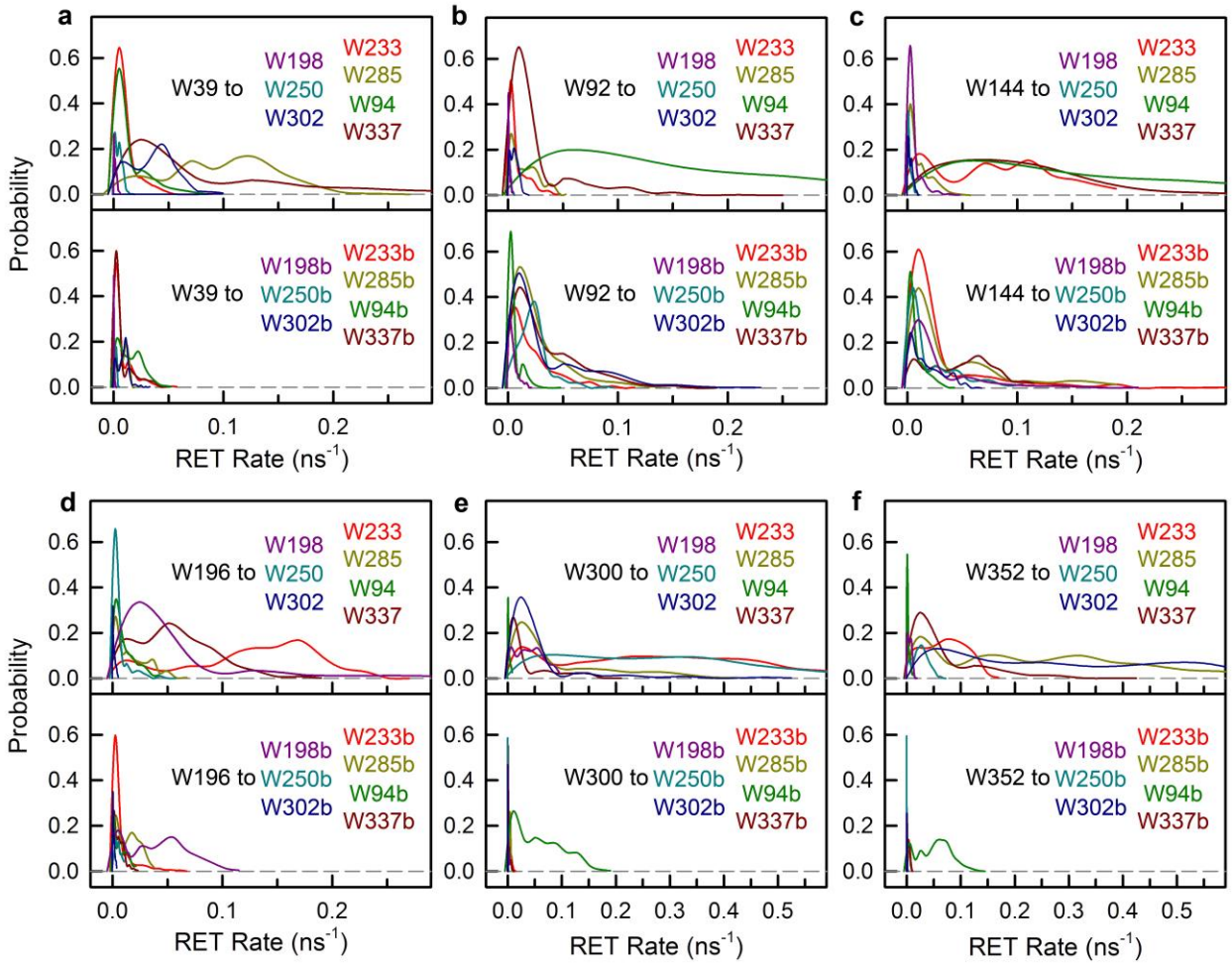

Supplementary Figure 5 | RET rate distributions for all 84 W_d to W_p/W_c donor-acceptor pairs based on QM/MM calculations. a, W39 as the donor. **b**, W92 as the donor. **c**, W144 as the donor. **d**, W196 as the donor. **e**, W300 as the donor. **f**, W352 as the donor. Top panels: energy transfer to tryptophan residues on the same subunit. Bottom panels: energy transfer to tryptophan residues on the other subunit.

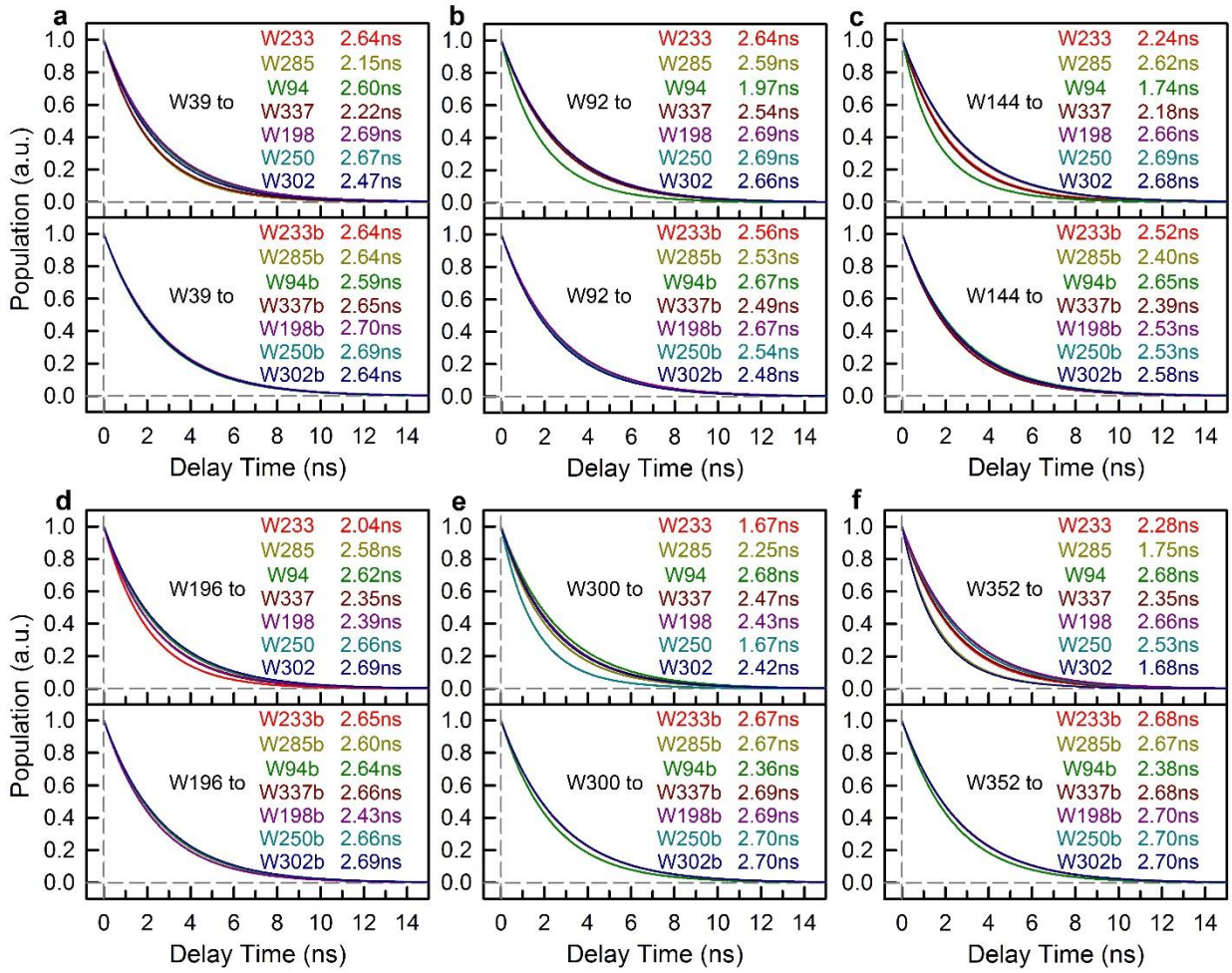

Supplementary Figure 6 | Simulated excited state decay dynamics of W_d in the presence of each individual energy acceptor. a, W39 as the donor. **b**, W92 as the donor. **c**, W144 as the donor. **d**, W196 as the donor. **e**, W300 as the donor. **f**, W352 as the donor. Top panels: energy transfer to tryptophan residues on the same subunit. Bottom panels: energy transfer to tryptophan residues on the other subunit.

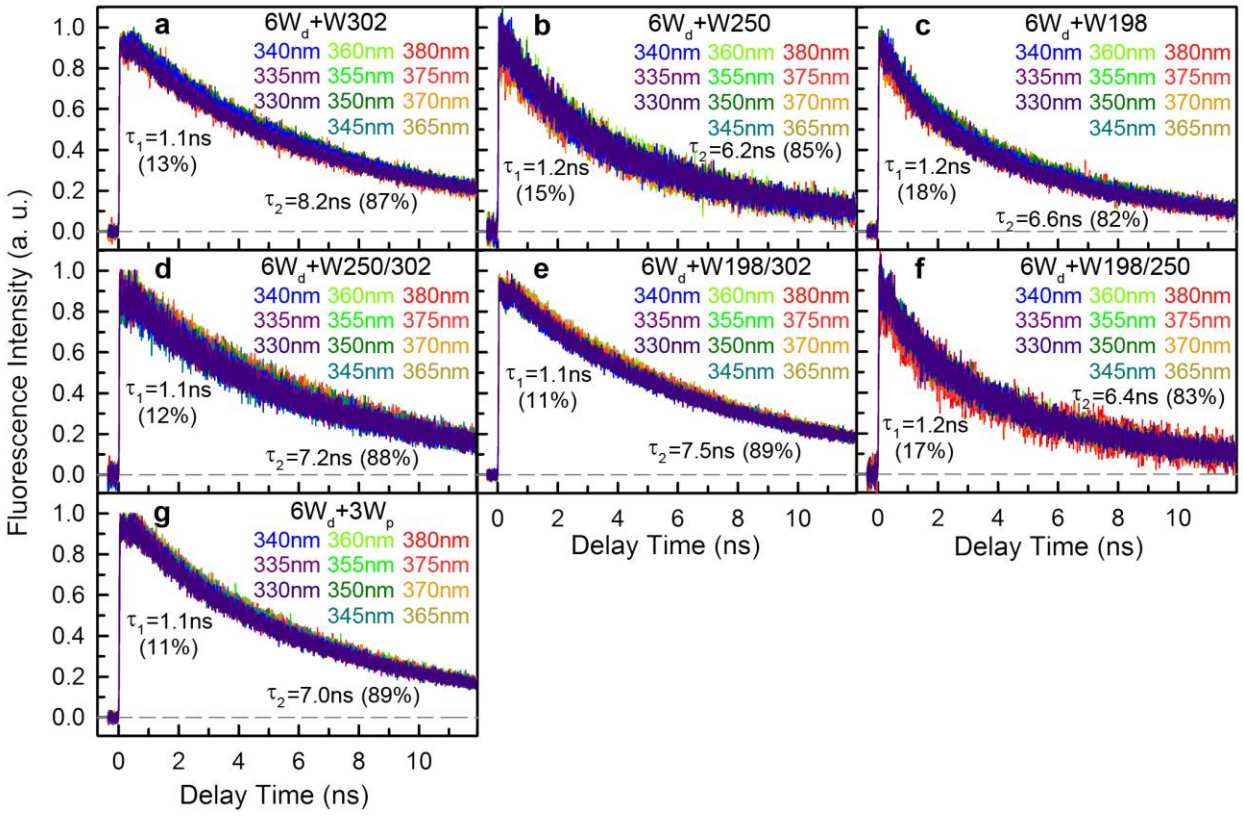

Supplementary Figure 7 | Fluorescence decay transients (λ_{ex}=310 nm) from 330 nm to 380 nm for 8 mutants measured with picosecond resolved time correlated single photon counting (TCSPC). a, 4W$_c$/198/250F (6W$_d$+W302); **b**, 4W$_c$/198/302F (6W$_d$+W250); **c**, 4W$_c$/250/302F (6W$_d$+W198); **d**, 4W$_c$/198F (6W$_d$+W250/302); **e**, 4W$_c$/250F (6W$_d$+W198/302); **f**, 4W$_c$/302F (6W$_d$+W198/250); **g**, 6W$_d$+3W$_p$. All these mutants contain 6W$_d$ and various W$_p$. For all mutants, transients at different wavelengths are very similar. Fitting results are shown for each mutant.

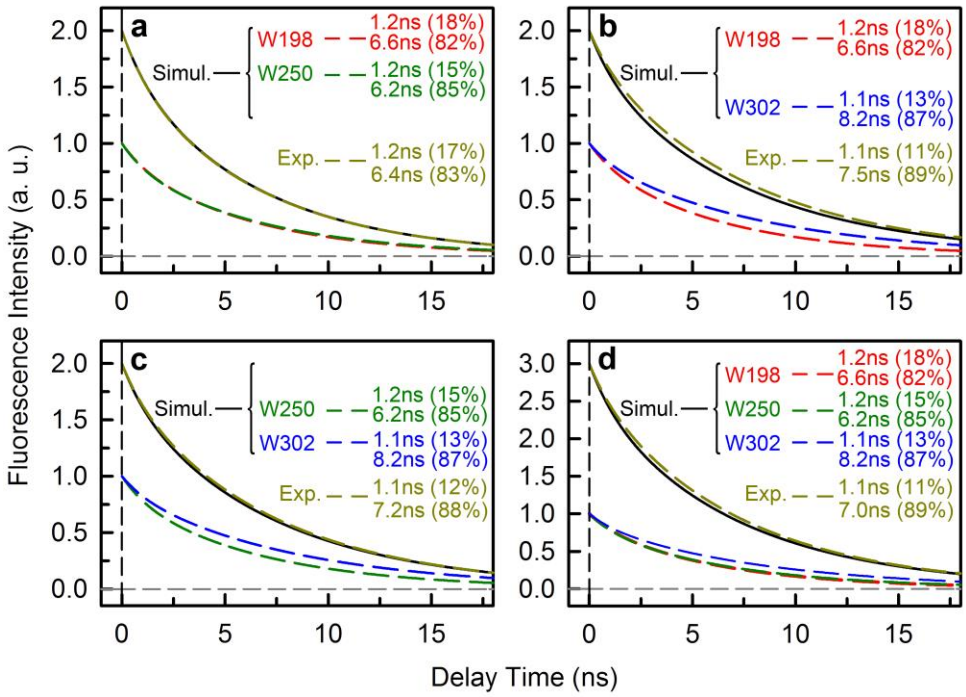

Supplementary Figure 8 | Numerical simulations show that the W_p lifetimes observed in $6W_d+2W_p$ mutants and $6W_d+3W_p$ mutants match the sum of decay transients of $6W_d+1W_p$. The mutants: **a**, $4W_c$/198F ($6W_d$+W250/302); **b**, $4W_c$/250F ($6W_d$+W198/302); **c**, $4W_c$/302F ($6W_d$+W198/250); **d**, $6W_d+3W_p$. For each mutant, decay transients of individual W_p (colored dashed lines, red-W198; green-W250; blue-W302) were simulated using double exponential decay model with the time constants and amplitude ratios (shown at the right side of the legend) measured from $6W_d+1W_p$ mutants, which add up a total decay transient (black solid line). The total transients agree with the simulated curves (orange solid lines) using time constants and ratios (shown in Supplementary Fig. 4) directly measured in "$6W_d+2W_p$" and "$6W_d+3W_p$" mutants.

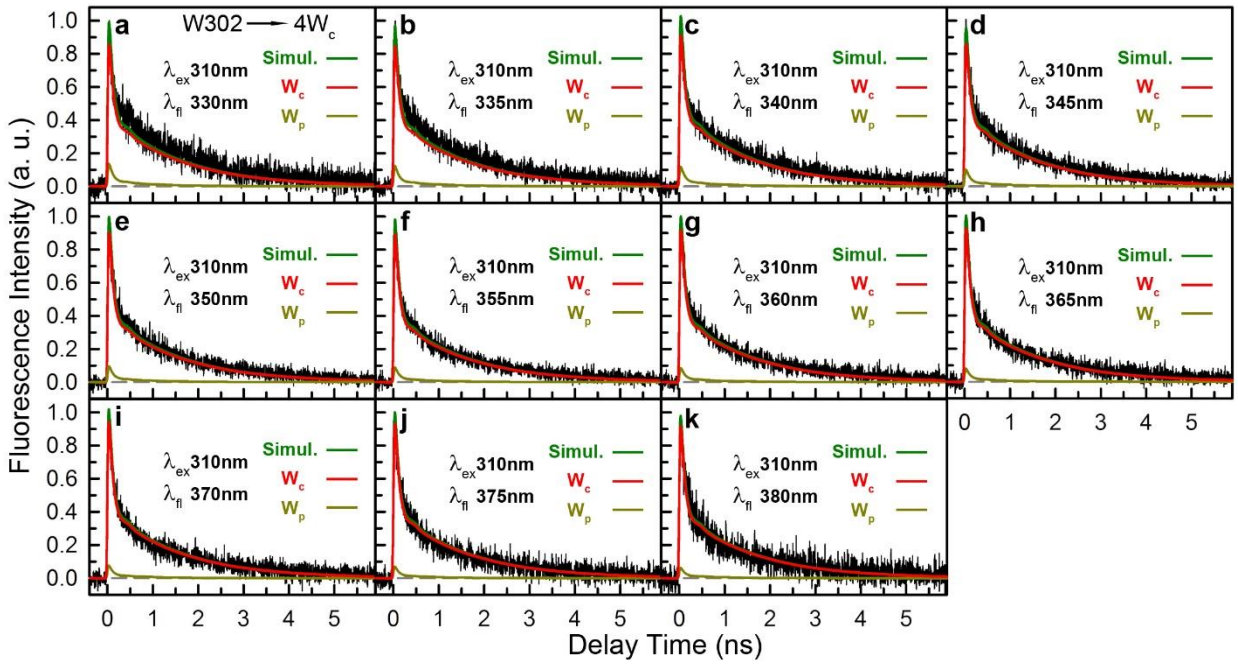

Supplementary Figure 9 | Fluorescence decay transients (λ_{ex}=310 nm) for W198/250F measured with picosecond-resolved TCSPC agree with model simulations. Transients were taken at various fluorescence wavelengths: **a**, 330 nm; **b**, 335 nm; **c**, 340 nm; **d**, 345 nm; **e**, 350 nm; **f**, 355 nm; **g**, 360 nm; **h**, 365 nm; **i**, 370 nm; **j**, 375 nm; and **k**, 380 nm. For each wavelength, the total simulated curve (green) and contributions from different tryptophan groups ($4W_c$, red; $3W_p$, dark yellow) are shown.

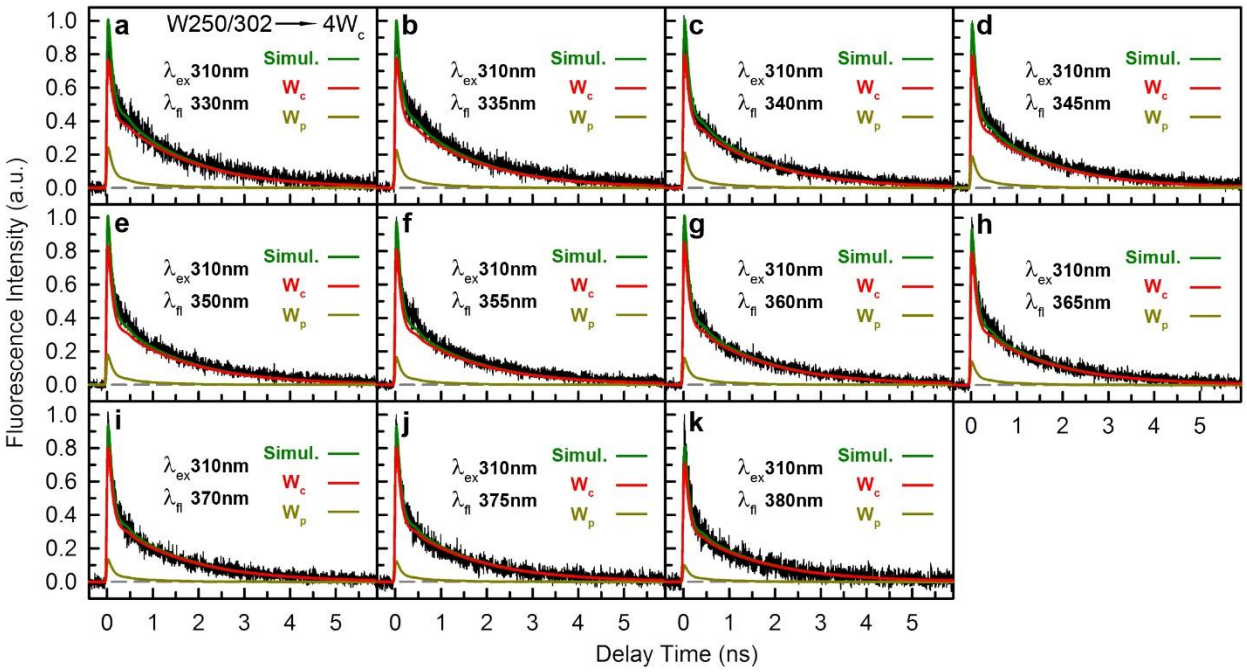

Supplementary Figure 10 | Fluorescence decay transients (λ_{ex}=310 nm) for W198F measured with picosecond-resolved TCSPC agree with model simulations. Transients were taken at various fluorescence wavelengths: **a**, 330 nm; **b**, 335 nm; **c**, 340 nm; **d**, 345 nm; **e**, 350 nm; **f**, 355 nm; **g**, 360 nm; **h**, 365 nm; **i**, 370 nm; **j**, 375 nm; and **k**, 380 nm. For each wavelength, the total simulated curve (green) and contributions from different tryptophan groups ($4W_c$, red; $3W_p$, dark yellow) are shown.

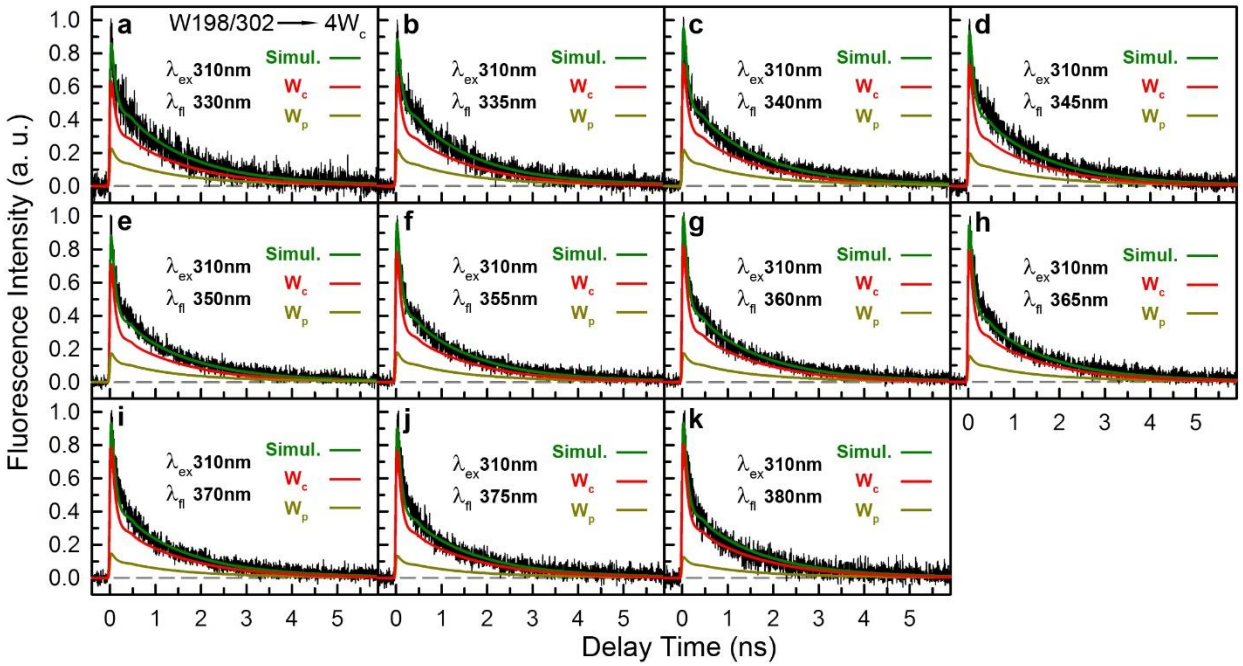

Supplementary Figure 11 | Fluorescence decay transients (λ_{ex}=310 nm) for W250F measured with picosecond-resolved TCSPC agree with model simulations. Transients were taken at various fluorescence wavelengths: **a**, 330 nm; **b**, 335 nm; **c**, 340 nm; **d**, 345 nm; **e**, 350 nm; **f**, 355 nm; **g**, 360 nm; **h**, 365 nm; **i**, 370 nm; **j**, 375 nm; and **k**, 380 nm. For each wavelength, the total simulated curve (green) and contributions from different tryptophan groups (4W_c, red; 3W_p, dark yellow) are shown.

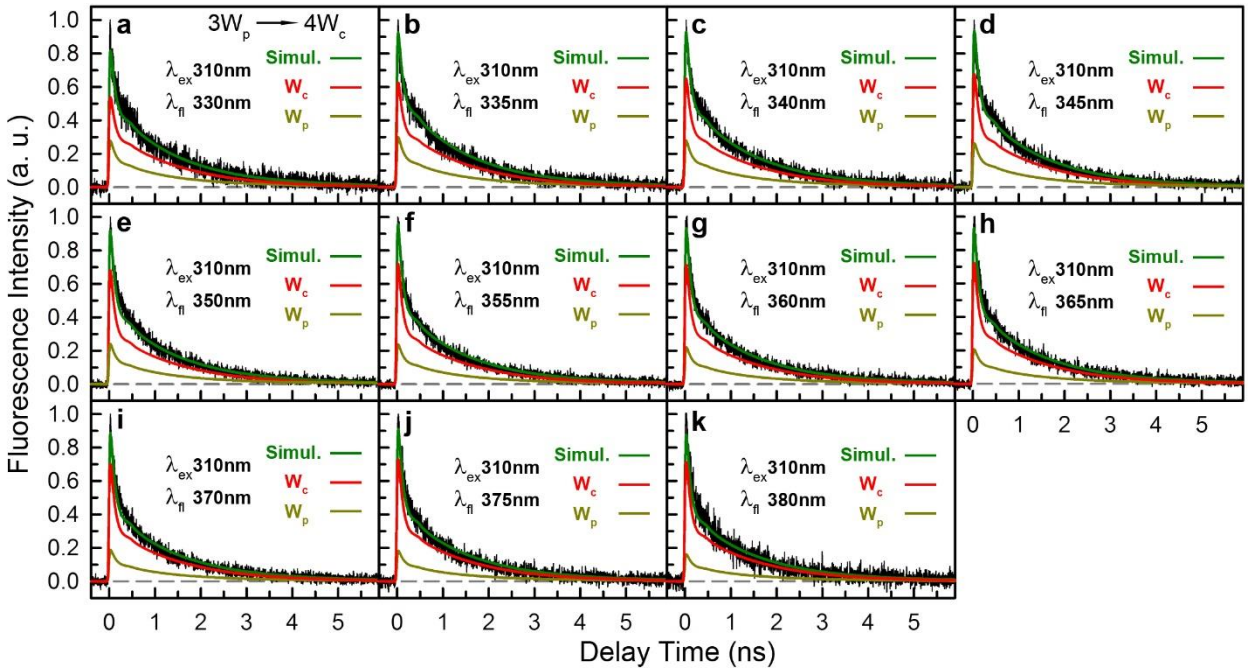

Supplementary Figure 12 | Fluorescence decay transients (λ_{ex}=310 nm) for WT measured with picosecond-resolved TCSPC agree with model simulations. Transients were taken at various fluorescence wavelengths: **a**, 330 nm; **b**, 335 nm; **c**, 340 nm; **d**, 345 nm; **e**, 350 nm; **f**, 355 nm; **g**, 360 nm; **h**, 365 nm; **i**, 370 nm; **j**, 375 nm; and **k**, 380 nm. For each wavelength, the total simulated curve (green) and contributions from different tryptophan groups ($4W_c$, red; $3W_p$, dark yellow) are shown.

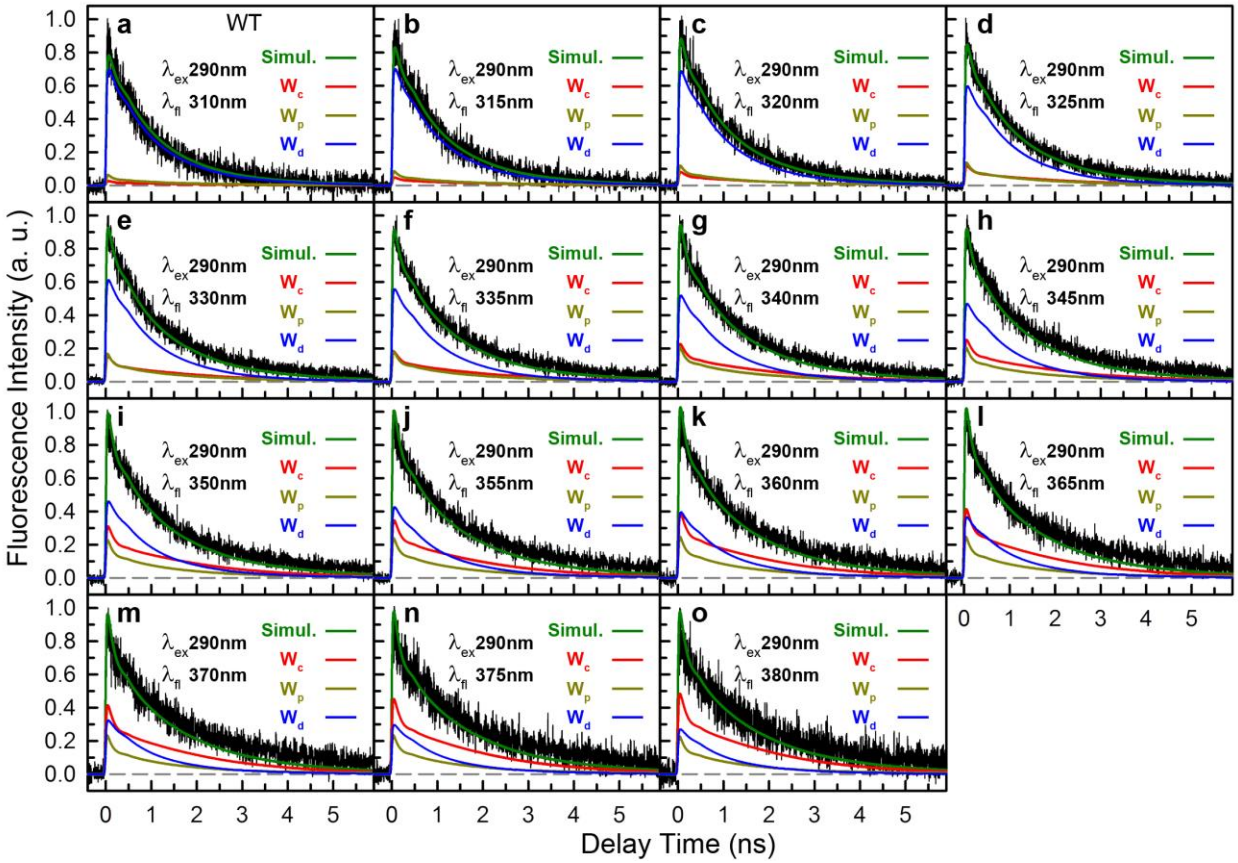

Supplementary Figure 13 | Fluorescence decay transients (λ_{ex}=290 nm) for WT measured with picosecond-resolved TCSPC agree with model simulations. Transients were taken at various fluorescence wavelengths: **a**, 310 nm; **b**, 315 nm; **c**, 320 nm; **d**, 325 nm; **e**, 330 nm; **f**, 335 nm; **g**, 340 nm; **h**, 345 nm; **i**, 350 nm; **j**, 355 nm; **k**, 360 nm; **l**, 365 nm; **m**, 370 nm; **n**, 375 nm; and **o**, 380 nm. For each wavelength, the total simulation curve (green) and contributions from different tryptophan groups ($4W_c$, red; $3W_p$, dark yellow; $6W_d$, blue) are shown. All simulation curves agree with experiments.

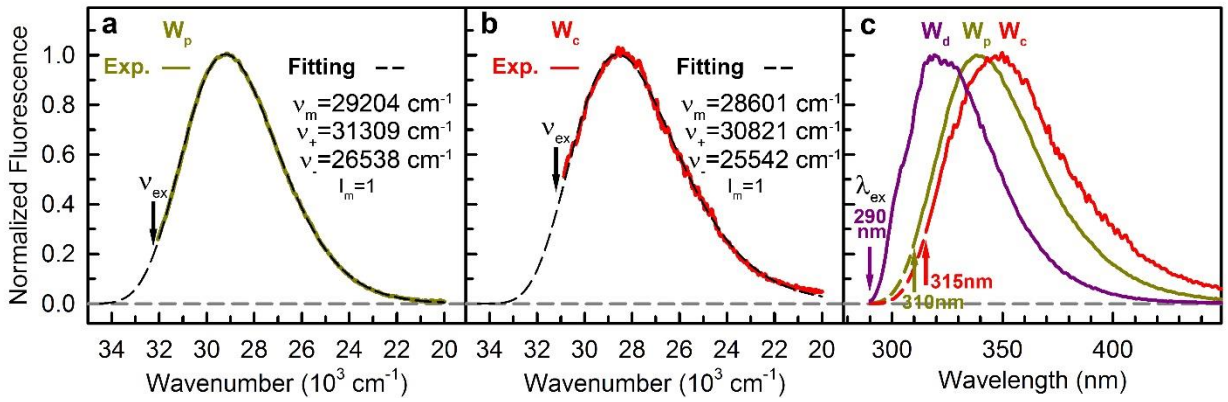

Supplementary Figure 14 | Blue sides of the emission spectra extended by log-normal fitting. **a**, W_p emission spectra (in frequency domain) measured with 310 nm (32258 cm^{-1}) excitation is shown in dark yellow. The log-normal fitting curve is shown in a black dashed line. The four fitting parameters were labeled. **b**, W_c emission spectra (in frequency domain) measured with 315 nm (31746 cm^{-1}) excitation is shown in red. The log-normal fitting curve is shown in a black dashed line. The four fitting parameters were labeled. **c**, Emission spectra of W_d, W_p and W_c in wavelength domain extended to 290 nm. The short-wavelength part from fitting are shown in dashed lines.

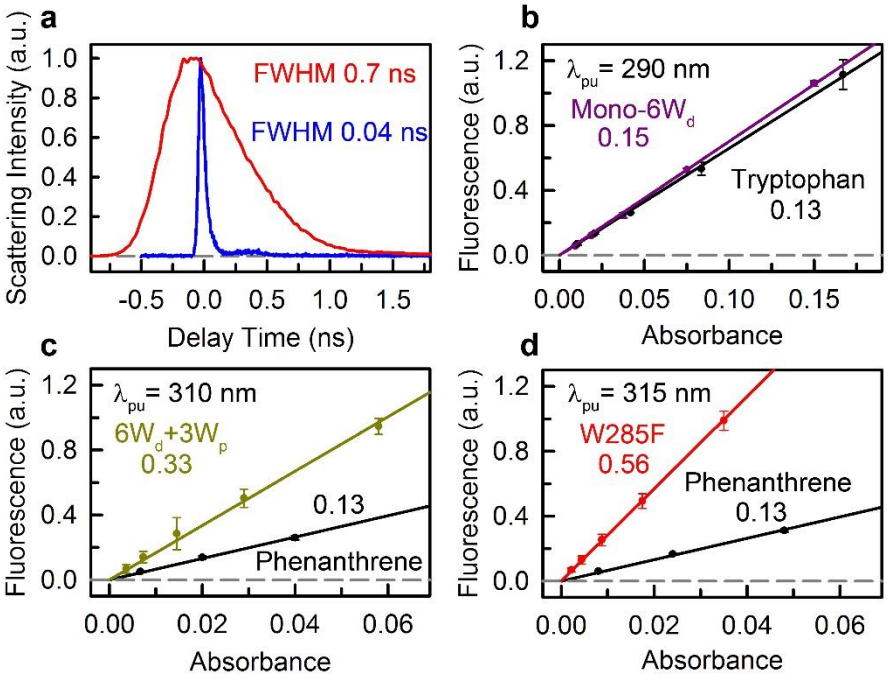

Supplementary Figure 15 | Instrument response functions of TCSPC and fluorescence quantum yields of three tryptophan groups. a, Instrument response functions for sub-nanosecond (red) and picosecond (blue) resolved TCSPC for data fitting and simulations. **b**, Fluorescence quantum yield of $6W_d$ as measured with mono-$6W_d$ (290 nm excitation) using tryptophan in aqueous solution as the standard. Radiative lifetime of W_d is about 14 ns, as calculated with the fluorescence QY and lifetime. **c**, Fluorescence quantum yield of $3W_p$ as measured with $6W_d$+$3W_p$ (310 nm excitation) using phenanthrene in absolute ethanol as the standard. Radiative lifetime of W_p is about 19 ns. **d**, Fluorescence quantum yield of pyramid center (W_c) without quenching as measured with W285F (315 nm excitation) using phenanthrene in absolute ethanol as the standard. The photoreaction was abolished by W285 mutation. Radiative lifetime of W_c is about 20 ns.

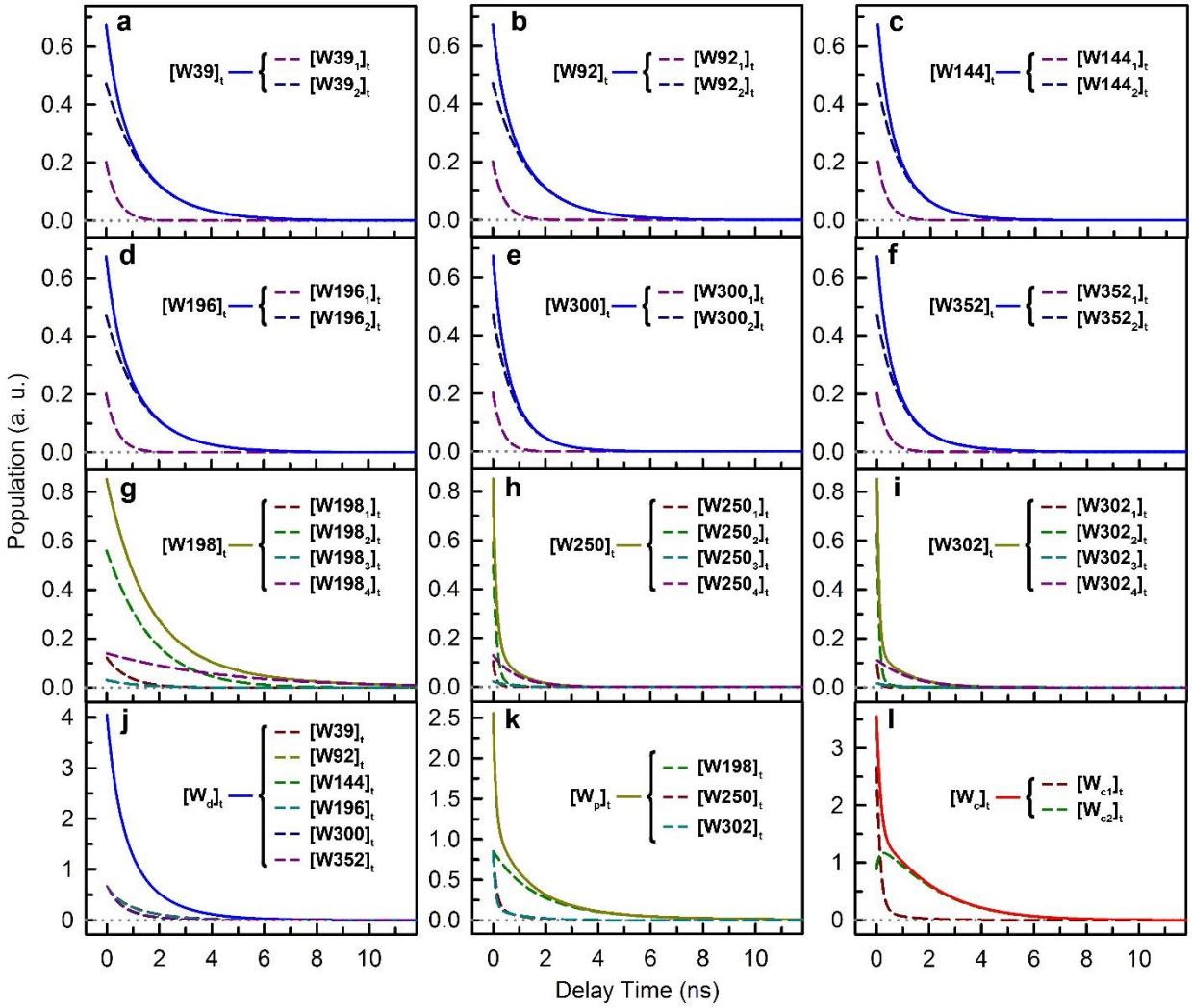

Supplementary Figure 16 | Excited state population evolution of various W residues and W groups in WT at 290-nm excitation obtained by numerical simulations. a, W39. **b**, W92. **c**, W144. **d**, W196. **e**, W300. **f**, W352. **g**, W198. **h**, W250. **i**, W302. **j**, $6W_d$ group. **k**, $3W_p$ group. **l**, $4W_c$ group. The temporal evolution for each W residue or group (solid lines) is the sum of population evolution curves of subpopulations or individual W residue in the group (dashed lines).

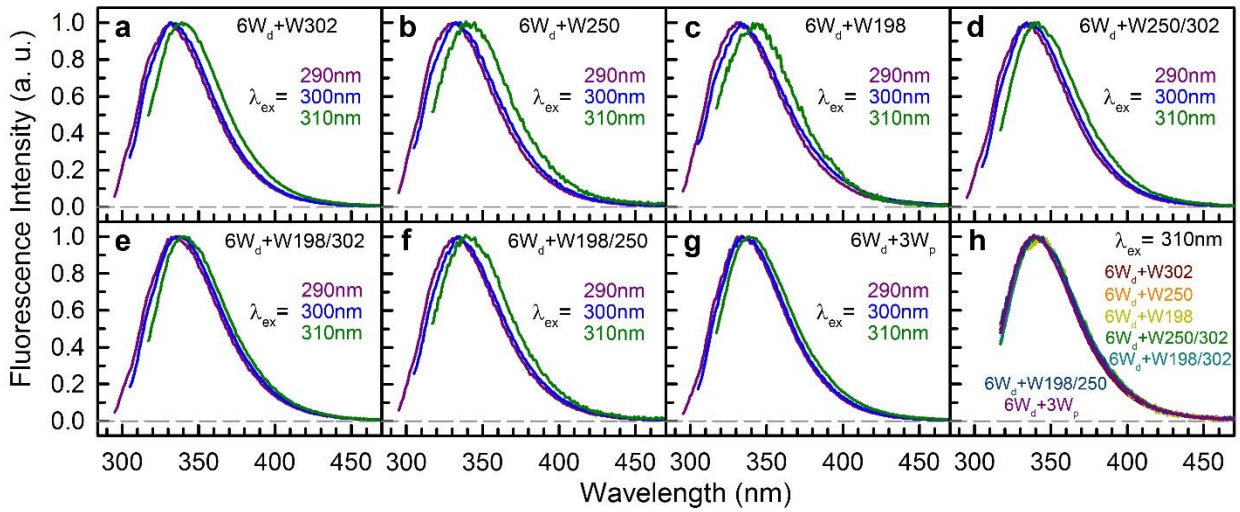

Supplementary Figure 17 | Steady-state emission spectra measured with various excitation wavelengths for UVR8 mutants containing the 6 distal tryptophan residues and various W_p. **a**, 4W_c/198/250F (6W_d+W302); **b**, 4W_c/198/302F (6W_d+W250); **c**, 4W_c/250/302F (6W_d+W198); **d**, 4W_c/198F (6W_d+W250/302); **e**, 4W_c/250F (6W_d+W198/302); **f**, 4W_c/302F (6W_d+W198/250); **g**, 6W_d+3W_p; **h**, Steady-state emission spectra (λ_{ex}=310 nm) for all the mutants are nearly identical, indicating that the 3 peripheral tryptophan (W_p) have similar emissions with peaks at around 340 nm.

Supplementary Tables

Supplementary Table 1 | Mutant summary

Mutant Type	Mutant	Abbreviated Name	State in Dark	UV Response
$6W_d$	W94/233/285/337/198/250F/W302H[†] /R286A[*]	mono-$6W_d$	Monomer	No
$6W_d$+$1W_p$	W94/233/285/337/198/250F	$4W_c$/ 198/250F	Dimer	No
	W94/233/285/337/198/302F	$4W_c$/ 198/302F	Dimer	No
	W94/233/285/337/250/302F	$4W_c$/ 250/302F	Dimer	No
$6W_d$+$2W_p$	W94/233/285/337/198F	$4W_c$/ 198F	Dimer	No
	W94/233/285/337/250F	$4W_c$/ 250F	Dimer	No
	W94/233/285/337/302F	$4W_c$/ 302F	Dimer	No
$6W_d$+$3W_p$	W94/233/285/337F	$6W_d$+$3W_p$	Dimer	No
$6W_d$+$4W_c$	W198/250/302F	$6W_d$+$4W_c$	Dimer	Yes
$6W_d$+$1W_p$+ $4W_c$	W198/250F	W198/250F	Dimer	Yes
$6W_d$+$2W_p$+ $4W_c$	W198F	W198F	Dimer	Yes
	W250F	W250F	Dimer	Yes

[†]W94/233/285/337/198/250F/W302H/R286A mutant has higher protein yield than the phenylalanine mutant W94/233/285/337/198/250F/W302F/R286A

[*]Mutation of all peripheral tryptophan residues without knocking out R286 leads to no protein yield.

Supplementary Table 2 | Overall RET efficiency of $6W_d$ in various systems.

Mutant Type	Mutant	RET Scheme	τ_{DA2} (ns) (Exp.)*	τ_{Ave} (ns) (Exp.)†	E (Exp.)¶
$6W_d+1W_p$	$4W_c$/ 198/250F	$6W_d$ to W302	2.42±0.1	23±10	0.08±0.03
	$4W_c$/ 198/302F	$6W_d$ to W250	2.37±0.1	19±6	0.10±0.03
	$4W_c$/ 250/302F	$6W_d$ to W198	2.29±0.1	15±4	0.12±0.04
$6W_d+2W_p$	$4W_c$/198F	$6W_d$ to W250/302	2.28±0.1	15±4	0.12±0.04
	$4W_c$/250F	$6W_d$ to W198/302	2.1±0.1	9.5±2	0.17±0.03
	$4W_c$/302F	$6W_d$ to W198/250	2.16±0.1	10.6±2	0.16±0.04
$6W_d+3W_p$	$6W_d+3W_p$	$6W_d$ to $3W_p$	1.94±0.1	6.9±1.5	0.22±0.04
$6W_d+4W_c$	$6W_d+4W_c$	$6W_d$ to $4W_c$	1.50±0.1	3.4±0.5	0.35±0.03
WT	WT	$6W_d$ to $3W_p+4W_c$	1.20±0.1	2.2±0.3‡	0.45±0.03

*Experimental τ_{DA2} measured with nanosecond resolved TCSPC (Fig. 2b-f and Supplementary Fig. 2a-d). Fitting error is 0.1 ns.

†Obtained using experimental τ_{DA2} and 2.7 ns ($1/(1/\tau_{DA2}-1/2.7)$. Errors were estimated based on 0.1 ns fitting errors of experimental τ_{DA2}.

¶Overall RET efficiency from $6W_d$ estimated with equations 20 to 22, assuming the experimental τ_{Ave} in column 5 as the RET time for each individual W_d.

‡RET rate constant in WT matches the value (2.3 ns) calculated from $1/(1/6.9+1/3.4)$.

Supplementary Table 3 | Calculated FRET time scales for all donor-acceptor pairs

τ_{RET} (ns)* W_d to W_p/W_c	W39	W92	W144	W196	W300	W352
W94	72 (30)	7.3 (5.4)	4.9 (2050)	85 (3510)	344 (165)	362 (100)
W233	111 (5390)	115 (83)	13 (6.0)	8.3 (6.6)	4.4 (4.7)	15 (26)
W285	11 (6.3)	67 (56)	93 (106)	58 (36)	14 (16)	4.9 (3.1)
W337	13 (161)	43 (1680)	11 (21)	18 (84)	29 (358)	18 (294)
W94b	64 (181)	206 (100)	137 (35)	125 (65)	18 (11)	20 (12)
W233b	121 (71)	48 (89)	39 (10)	135 (60)	275 (302)	301 (165)
W285b	127 (988)	40 (13)	22 (100)	70 (44)	278 (187)	277 (236)
W337b	135(409000)	32 (13)	21 (9.3)	171 (147)	558 (7740)	329 (2400)
To Pyramid†	4.2 (4.6)	3.8 (2.6)	2.0 (2.1)	4.2 (3.9)	2.5 (2.6)	2.6 (2.2)
W198	660 (1550)	909(16100)	194 (120)	21 (9.3)	24 (10)	175 (139)
W250	212 (140)	726 (366)	483 (169)	175 (160)	4.4 (14)	39 (28)
W302	29 (26)	180 (112)	362 (170)	660 (588)	24 (138)	4.5 (7.3)
W198b	2430(30300)	218 (653)	40 (314)	25 (9.8)	726 (328)	2420(1440)
W250b	605 (504)	43 (39)	40 (998)	194 (296)	7290(4170)	8130(2100)
W302b	115 (101)	30 (97)	59 (647)	908 (109000)	7320(1910)	1460(745)
To peripheral§	19 (17)	15 (20)	13 (39)	9.8 (4.5)	3.2 (5.6)	3.9 (5.5)
τ_{total}**	3.6 (3.6)	3.1 (2.3)	1.7 (2.0)	3.0 (2.1)	1.4 (1.8)	1.8 (1.6)
FRET Branching Ratios¶ (Pyramid/Peripheral)	3.7	8.0	18	1.1	2.2	2.6

τ_{RET} (ns)* W_p to W_c	W198	W250	W302
W94b	14.0	2.1	5.7
W233	3.2	0.12	44.4
W285	45.7	0.63	0.05
W337	12.0	518	2.3
τ_{total}**	2.0	0.1	0.05

*τ_{RET} values for W_d to W_p/W_c were effective RET times defined using equation 15 based on 500 MD simulation snapshots. Values in brackets were calculated with supplementary equation 9 based on X-ray structure. τ_{RET} values for W_p to W_c were calculated with supplementary equation 9 based on X-ray structure.

†Total FRET time constants of the parallel 8 energy transfers to the 8 pyramid center W residues ($4W_c$ on both subunits).

§Total FRET time constants of the parallel 6 energy transfers to the 6 peripheral W residues ($3W_p$ on both subunits).

**Total energy transfer time scale for all parallel energy transfer pathways.

¶Obtained by dividing total peripheral FRET time constants by total pyramid FRET time constants.

Supplementary Table 4 | Energy transfer efficiency of W_p and W_d

	W198	W250	W302
Fast energy transfer time constant (τ_{total1})	1.8 ns	0.12 ns	0.08 ns
Slow energy transfer time constant (τ_{total2})	12.3 ns	1.0 ns	1.1 ns
Population ratio of slow energy transfer (R_{slow})	0.20	0.18	0.15
First lifetime (τ_1)	1.2 ns (18%)	1.2 ns (15%)	1.1 ns (13%)
Second lifetime (τ_2)	6.6 ns (82%)	6.2 ns (85%)	8.2 ns (87%)
Energy transfer efficiency to $4W_c$*	0.63	0.94	0.96
Overall efficiency $3W_p$ to $4W_c$	0.84		

	W39	W92	W144	W196	W300	W352
Total RET efficiency (E)*	0.35	0.38	0.50	0.38	0.54	0.52
Overall efficiency $6W_d$ to $3W_p$+$4W_c$	0.44					
Efficiency of direct transfer to $4W_c$ ($E_{direct,4Wc}$)†	0.28	0.30	0.43	0.27	0.31	0.31
Efficiency to W198 (E_{W198})§	<0.01	0.01	0.03	0.10	0.03	<0.01
Efficiency to W250 (E_{W250})§	0.01	0.03	0.02	0.01	0.17	0.02
Efficiency to W302 (E_{W302})§	0.05	0.04	0.02	<0.01	0.03	0.18
Efficiency to $4W_c$ via W_p ($E_{twostep}$)¶	0.06	0.07	0.05	0.08	0.21	0.20
Total RET efficiency to the pyramid center (E_{4Wc})‡	0.34	0.37	0.49	0.35	0.52	0.51
Overall efficiency $6W_d$ to $4W_c$	0.43					

*The fraction of W_d excited energy that is transferred to interfacial W residues.

†The fraction of W_d excited energy that is directly transferred to the pyramid center.

§The fraction of W_d excited energy that is transferred to each of the $3W_p$.

¶The fraction of W_d excited energy that is transferred to the pyramid center via $3W_p$.

‡The fraction of W_d excited energy that is transferred to the pyramid center, both directly and indirectly. The values are smaller than the total efficiency, meaning that a small fraction of energy dissipates in the two-step channels via W_p.

Supplementary Table 5 | A_d, A_p and A_c values used in model simulations and excitation population percentage calculations.

A_d(310 nm)	A_p(310 nm)	A_c(310 nm)	A_d(290 nm)	A_p(290 nm)	A_c(290 nm)
0	0.044	0.109	0.668	0.846	0.888

The values are direct readings of absorption curves in Fig. 1e. Initial excited populations of tryptophan residues are proportional to absorbance values, thus, we used the absorbance values as the initial populations in our model simulations. The same A_d value was used for all the 6 different W_d. The same A_p value was used for W198, W250 and W302. In mutants where certain W_p were knocked out, the A_p value for the corresponding W_p was set to 0 in our simulations. For 290 nm excitation, excited state population distributions among three groups can be calculated with absorbance values: W_d, (0.668*6)/(0.668*6+0.846*3+0.888*4)=40%; W_p (0.846*3)/(0.668*6+0.846*3+0.888*4)=25%; W_c, (0.888*4)/(0.668*6+0.846*3+0.888*4)=35%.

Supplementary Table 6 | Fitting parameters for sub-nanosecond TCSPC transients of $4W_c/198/250F$ ($6W_d$+W302) with the multiple-exponential decay model (equation 5).

Fluorescence Wavelength (nm)	Amplitude Percentage for Different Time Constants		
	0.5 ns	2.43 ns	8.21 ns
305	49.8	47.6	2.6
310	45.2	51.0	3.8
315	38.7	55.3	6.0
320	34.3	57.0	8.7
325	30.4	57.9	11.7
330	25.5	59.3	15.3
335	23.0	57.8	19.2
340	19.6	57.3	23.1
345	17.1	55.6	27.4
350	13.0	55.1	31.9
355	10.2	53.2	36.6
360	8.1	51.2	40.6
365	8.3	47.7	44.1
370	0.6	48.4	51.0
375	3.0	44.3	52.7
380	0.2	43.0	56.8

Supplementary Table 7 | Fitting parameters for sub-nanosecond TCSPC transients of $4W_c/198/302F$ ($6W_d$+W250) with the multiple-exponential decay model (equation 5).

Fluorescence Wavelength (nm)	Amplitude Percentage for Different Time Constants		
	0.5 ns	2.41 ns	6.23 ns
305	36.8	58.1	5.0
310	33.1	60.0	6.9
315	28.8	61.5	9.6
320	25.4	62.0	12.6
325	21.2	62.8	16.1
330	20.4	60.4	19.2
335	16.9	60.0	23.1
340	17.7	56.3	26.0
345	15.0	55.0	30.0
350	16.4	51.0	32.6
355	13.3	50.3	36.4
360	12.7	47.7	39.6
365	14.3	43.9	41.9
370	9.8	44.2	46.0
375	13.8	39.2	47.0
380	12.2	37.9	49.9

Supplementary Table 8 | Fitting parameters for sub-nanosecond TCSPC transients of $4W_c/250/302F$ ($6W_d$+W198) with the multiple-exponential decay model (equation 5).

Fluorescence Wavelength (nm)	Amplitude Percentage for Different Time Constants		
	0.5 ns	2.18 ns	6.58 ns
305	33.8	60.9	5.3
310	32.1	60.9	7.0
315	28.7	62.0	9.3
320	26.7	61.2	12.1
325	25.6	59.1	15.3
330	21.0	60.2	18.8
335	18.8	58.6	22.6
340	17.1	56.3	26.6
345	17.4	52.8	29.8
350	14.2	51.2	34.6
355	13.0	48.5	38.5
360	12.7	45.3	42.1
365	10.3	44.0	45.7
370	11.7	39.5	48.7
375	9.6	38.4	51.9
380	7.7	36.8	55.5

Supplementary Table 9 | Fitting parameters for sub-nanosecond TCSPC transients of $4W_c/198F$ ($6W_d$+W250/302) with the multiple-exponential decay model (equation 5).

Fluorescence Wavelength (nm)	Amplitude Percentage for Different Time Constants		
	0.5 ns	2.28 ns	7.15 ns
305	41.1	55.3	3.6
310	39.5	54.6	6.0
315	37.2	53.5	9.3
320	29.1	56.7	14.2
325	28.9	52.7	18.5
330	26.2	50.4	23.4
335	23.5	47.7	28.8
340	21.0	44.7	34.3
345	18.9	41.4	39.7
350	16.8	38.2	45.0
355	15.8	34.8	49.5
360	14.2	31.5	54.2
365	12.9	28.5	58.5
370	12.3	24.8	62.8
375	10.0	22.9	67.1
380	11.1	18.9	70.0

Supplementary Table 10 | Fitting parameters for sub-nanosecond TCSPC transients of $4W_c/250F$ ($6W_d$+W198/302) with the multiple-exponential decay model (equation 5).

Fluorescence Wavelength (nm)	Amplitude Percentage for Different Time Constants		
	0.5 ns	2.10 ns	7.54 ns
305	42.5	53.3	4.2
310	38.1	55.1	6.8
315	35.0	54.1	10.9
320	29.1	55.3	15.7
325	27.4	51.6	21.0
330	24.6	48.6	26.8
335	22.3	45.2	32.5
340	19.7	41.5	38.8
345	17.2	37.5	45.3
350	15.2	33.8	50.9
355	14.7	29.4	55.9
360	12.9	25.2	61.8
365	11.0	21.8	67.2
370	10.0	17.4	72.6
375	9.8	14.6	75.6
380	11.3	9.5	79.2

Supplementary Table 11 | Fitting parameters for sub-nanosecond TCSPC transients of $4W_c/302F$ ($6W_d$+W198/250) with the multiple-exponential decay model (equation 5).

Fluorescence Wavelength (nm)	Amplitude Percentage for Different Time Constants		
	0.5 ns	2.15 ns	6.36 ns
305	39.2	55.4	5.4
310	35.4	56.2	8.4
315	32.7	56.1	11.1
320	27.4	57.4	15.2
325	23.7	56.7	19.6
330	21.5	54.8	23.7
335	18.0	54.4	27.6
340	15.4	52.6	32.1
345	10.6	52.4	37.0
350	11.3	48.8	39.9
355	9.6	46.8	43.6
360	6.6	45.5	47.8
365	7.7	41.8	50.5
370	5.4	40.6	54.0
375	2.5	39.8	57.6
380	2.0	38.0	60.0

Supplementary Table 12 | Fitting parameters for sub-nanosecond TCSPC transients of $6W_d+3W_p$ with the multiple-exponential decay model (equation 5).

Fluorescence Wavelength (nm)	Amplitude Percentage for Different Time Constants		
	0.5 ns	1.94 ns	6.98 ns
305	23.2	68.5	8.3
310	23.2	64.2	12.6
315	18.4	61.9	19.7
320	19.0	56.0	25.0
325	18.3	50.9	30.8
330	16.9	46.0	37.1
335	13.5	43.4	43.1
340	11.1	38.9	50.0
345	8.5	35.2	56.2
350	4.8	32.9	62.3
355	8.1	26.9	65.0
360	6.8	24.2	69.0
365	7.0	20.4	72.6
370	9.0	15.1	75.9
375	5.4	13.3	81.3
380	7.0	9.9	83.1

Supplementary Table 13 | Fitting parameters for sub-nanosecond TCSPC transients of $6W_d+4W_c$ with the multiple-exponential decay model (equation 5).

Fluorescence Wavelength (nm)	Amplitude Percentage for Different Time Constants			
	0.45 ns	1.50 ns	1.42 ns	5.41 ns
305	58.3	39.5	0.8	1.4
310	51.2	45.8	1.1	1.9
315	49.6	46.7	1.3	2.4
320	46.1	49.2	1.7	3.0
325	46.0	48.8	1.6	3.6
330	45.2	49.0	1.6	4.2
335	43.7	47.1	4.4	4.9
340	43.0	44.8	6.7	5.5
345	43.7	42.2	8.1	5.9
350	41.2	41.6	10.7	6.6
355	43.4	37.0	12.9	6.6
360	43.5	32.4	17.3	6.8
365	42.3	29.2	21.4	7.1
370	45.5	27.4	19.7	7.4
375	45.4	24.9	22.5	7.1
380	43.4	22.5	26.6	7.5

Supplementary Table 14 | Fitting parameters for sub-nanosecond TCSPC transients of WT with multiple-the exponential decay model (equation 5).

Fluorescence Wavelength (nm)	Amplitude Percentage for Different Time Constants			
	0.45 ns	1.18 ns	1.4 ns	6.9 ns
305	58.7	38.2	2.2	0.9
310	59.6	30.3	9.4	0.7
315	53.8	35.6	9.6	1.1
320	52.7	33.5	12.4	1.3
325	53.4	29.9	15.2	1.5
330	50.9	29.3	17.9	1.9
335	49.2	29.8	18.8	2.3
340	50.5	25.6	21.1	2.7
345	48.9	23.8	24.7	2.6
350	44.9	23.9	27.4	3.8
355	49.9	18.9	28.0	3.2
360	49.5	17.1	30.4	3.0
365	44.7	17.7	33.6	4.0
370	45.7	16.9	33.6	3.9
375	40.3	16.3	38.7	4.7
380	43.3	16.0	35.4	5.3

Supplementary Table 15 | Distances and κ^2 between distal and interfacial tryptophan residues.

R (Å)	W39	W92	W144	W196	W300	W352
W94	20.5	14.1	14.9	21.8	28.3	26.0
W198	29.7	26.8	20.1	13.6	20.7	27.0
W233	21.7	21.1	18.9	17.2	17.1	19.7
W250	27.4	28.8	25.6	19.8	14.3	21.3
W285	19.4	21.6	22.3	21.7	16.0	16.4
W302	21.1	26.8	28.8	27.1	14.0	14.1
W337	16.7	17.4	18.6	20.0	17.3	16.2
W94b	23.3	23.8	23.9	23.8	21.5	21.9
W198b	32.9	25.2	18.7	20.6	33.9	35.9
W233b	27.0	21.0	19.6	24.2	32.0	31.1
W250b	30.8	21.6	18.8	25.9	38.1	37.0
W285b	24.3	18.4	20.1	27.0	33.0	30.1
W302b	25.2	18.0	22.1	31.5	38.2	33.6
W337b	24.7	21.0	22.6	27.6	31.4	28.9
κ^2	W39	W92	W144	W196	W300	W352
W94	0.46	0.27	0.00	0.01	0.58	0.57
W198	0.16	0.01	0.20	0.25	2.71	1.01
W233	0.00	0.20	1.42	0.73	0.98	0.42
W250	1.09	0.56	0.61	0.14	0.22	1.17
W285	1.58	0.34	0.22	0.55	0.20	1.15
W302	1.25	1.20	1.20	0.24	0.02	0.40
W337	0.02	0.00	0.37	0.14	0.01	0.01
W94b	0.17	0.34	0.99	0.53	1.70	1.69
W198b	0.02	0.14	0.05	2.80	1.67	0.53
W233b	1.03	0.18	1.00	0.63	0.66	1.03
W250b	0.61	0.94	0.02	0.37	0.26	0.44
W285b	0.04	0.57	0.12	1.64	1.30	0.59
W302b	0.92	0.13	0.06	0.00	0.59	0.70
W337b	0.00	1.21	2.64	0.56	0.02	0.05

All results were based on X-ray structures[16,17]. We used the midpoint of the C_{3a}-C_{7a} bond of indole ring as the center of the indole chromophores for distance calculations.

Supplementary Table 16 | κ^2/R^6 between distal ($6W_d$) and interfacial tryptophan residues ($3W_p$ and $4W_c$) for all donor-acceptor pairs.

κ^2/R^6 (10^{-9}Å^{-6})	W39	W92	W144	W196	W300	W352
W94	6.28	34.50	0.09	0.05	1.13	1.87
W198	0.23	0.02	3.01	38.90	34.70	2.60
W233	0.03	2.26	31.20	28.40	39.60	7.19
W250	2.58	0.99	2.14	2.26	25.80	12.70
W285	29.50	3.35	1.77	5.21	12.00	59.80
W302	14.00	3.22	2.13	0.61	2.62	49.40
W337	1.16	0.11	9.12	2.22	0.52	0.64
To A*	53.76	44.40	49.50	77.70	116.00	134.00
W94b	1.03	1.87	5.36	2.88	17.00	15.30
W198b	0.01	0.55	1.15	36.80	1.10	0.25
W233b	2.62	2.09	17.90	3.10	0.62	1.13
W250b	0.72	9.18	0.36	1.22	0.09	0.17
W285b	0.19	14.60	1.86	4.27	1.00	0.79
W302b	3.56	3.73	0.56	0.00	0.19	0.49
W337b	0.00	14.20	20.00	1.27	0.02	0.08
To B†	8.14	46.20	47.20	49.60	20.10	18.20

*Sum of the 7 κ^2/R^6 values to the interfacial W residues on the same subunit as the distal tryptophan donor.

†Sum of the 7 κ^2/R^6 values to the interfacial W residues on the other subunit.

Supplementary Table 17 | Distances and κ^2/R^6 between $3W_p$ and $4W_c$.

R (Å)	W198	W250	W302
W94b	13.1	11.2	10.7
W233	8.6	8.2	11.5
W285	13.2	9.2	7.1
W337	13.9	12.3	10.7
W94	17.8	21.2	21.2
W233b	17.5	21.8	23.4
W285b	21.3	24.4	23.9
W337b	19.9	22.0	21.1
κ^2/R^6 (10^{-9}Å^{-6})	W198	W250	W302
W94b	70.5	478	172
W233	310	8250	22.2
W285	21.6	1560	19000
W337	82.3	19.1	421
To the closer pyramid*	485	10000	20000
W94	2.0	1.6	1.0
W233b	15.1	1.1	0.5
W285b	18.7	6.5	10.9
W337b	5.6	30	33.7
To the further pyramid†	41	39	46

Results were based on X-ray structures[16,17]. We used the midpoint of the C_{3a}-C_{7a} bond of indole ring as the center of the indole chromophores for distance calculations.

*Sum of the 4 κ^2/R^6 values to the closer $4W_c$.

†Sum of the 4 κ^2/R^6 values to the further $4W_c$.

Supplementary Table 18 | Lifetimes and amplitude ratios used in model simulations and energy transfer efficiency calculations.

Description	Symbol	Value
The first lifetime of W_d	τ_1	0.5 ns
The second lifetime of W_d	τ_2	2.7 ns
Amplitude ratio of the second lifetime of W_d	R_{D2}	0.71
The first lifetime of W198	$\tau_{1,W198}$	1.2 ns
The second lifetime of W198	$\tau_{2,W198}$	6.6 ns
Amplitude ratio of the second lifetime of W198	$R_{2,W198}$	0.82
Fast energy transfer time constant of W198	$\tau_{total1,W198}$	1.8 ns
Slow energy transfer time constant of W198	$\tau_{total2,W198}$	12.3 ns
Amplitude ratio of slow energy transfer in W198	$R_{slow,W198}$	0.20
The first lifetime of W250	$\tau_{1,W250}$	1.2 ns
The second lifetime of W250	$\tau_{2,W250}$	6.2 ns
Amplitude ratio of the second lifetime of W250	$R_{2,W250}$	0.85
Fast energy transfer time constant of W250	$\tau_{total1,W250}$	0.12 ns
Slow energy transfer time constant of W250	$\tau_{total2,W250}$	1.0 ns
Amplitude ratio of slow energy transfer in W250	$R_{slow,W250}$	0.18
The first lifetime of W302	$\tau_{1,W302}$	1.1 ns
The second lifetime of W302	$\tau_{2,W302}$	8.2 ns
Amplitude ratio of the second lifetime of W302	$R_{2,W302}$	0.87
Fast energy transfer time constant of W302	$\tau_{total1,W302}$	0.08 ns
Slow energy transfer time constant of W302	$\tau_{total2,W302}$	1.1 ns
Amplitude ratio of slow energy transfer in W302	$R_{slow,W302}$	0.15
The first fluorescence decay time of the pyramid center	τ_{c1}	0.08 ns
The second fluorescence decay time of the pyramid center	τ_{c2}	1.4 ns
Amplitude ratio of the 0.08 ns component	R_{c1}	0.75

Supplementary Table 19 | Values of FL_d, FL_p and FL_c at various wavelengths for model simulations.

Wavelength (nm)	FL_d (a.u.)	FL_p (a.u.)	FL_c (a.u.)
310	1.46	0.247	0.068
315	1.84	0.421	0.150
320	1.89	0.612	0.268
325	1.83	0.786	0.433
330	1.79	0.916	0.541
335	1.60	0.987	0.636
340	1.35	1	0.72
345	1.17	0.963	0.772
350	0.969	0.891	0.790
355	0.768	0.798	0.755
360	0.601	0.695	0.711
365	0.477	0.593	0.650
370	0.372	0.497	0.580
375	0.279	0.411	0.518
380	0.216	0.336	0.469

FL_d, FL_p and FL_c are the fluorescence intensity per unit population per unit time for excited W_d, W_p and W_c, respectively. Ratios of FL_d, FL_p and FL_c at various wavelengths give the weights of 3 tryptophan groups in total simulated signals (Supplementary equations 15, 16 and 17). For each group, plots of FL numbers versus wavelengths have the same shape as the emission spectrum of the tryptophan group shown in Fig. 1e. Their wavelength integrals were inversely proportional to the radiative lifetimes (inverse of radiative rates) of 3 W groups, which were estimated based on fluorescence quantum yields and lifetimes (Supplementary Fig. 15).

References

1. Andrews, D. L. & Demidov, A. A. Resonance Energy Transfer (Wiley, Chichester, England, 1999).